Inorganic Chemistry

Article

pubs.acs.org/IC

Model Peptide Studies Reveal a Mixed Histidine-Methionine Cu(I) Binding Site at the N-Terminus of Human Copper Transporter 1

M. Jake Pushie,[†,‡] Katharine Shaw,[§] Katherine J. Franz,[∥] Jason Shearer,[⊥] and Kathryn L. Haas*[,§]

[†]Department of Anatomy and Cell Biology, University of Saskatchewan, Saskatoon, Saskatchewan, Canada

[‡]Canadian Light Source Incorporated, Saskatoon, Saskatchewan, Canada

[§]Department of Chemistry and Physics, Saint Mary's College, Notre Dame, Indiana 46556, United States

[∥]Department of Chemistry, Duke University, Durham, North Carolina 27708, United States

[⊥]Department of Chemistry, University of Nevada, Reno, Nevada 895030, United States

Supporting Information

ABSTRACT: Copper is a vital metal cofactor in enzymes that are essential to myriad biological processes. Cellular acquisition of copper is primarily accomplished through the Ctr family of plasma membrane copper transport proteins. Model peptide studies indicate that the human Ctr1 N-terminus binds to Cu(II) with high affinity through an amino terminal Cu(II), Ni(II) (ATCUN) binding site. Unlike typical ATCUN-type peptides, the Ctr1 peptide facilitates the ascorbate-dependent reduction of Cu(II) bound in its ATCUN site by virtue of an adjacent HH (*bis*-His) sequence in the peptide. It is likely that the Cu(I) coordination environment influences the redox behavior of Cu bound to this peptide; however, the identity and coordination geometry of the Cu(I) site has not been elucidated from previous work. Here, we show data from NMR, XAS, and structural modeling that sheds light on the identity of the Cu(I) binding site of a Ctr1 model peptide. The Cu(I) site includes the same *bis*-His site identified in previous work to facilitate ascorbate-dependent Cu(II) reduction. The data presented here are consistent with a rational mechanism by which Ctr1 provides coordination environments that facilitate Cu(II) reduction prior to Cu(I) transport.

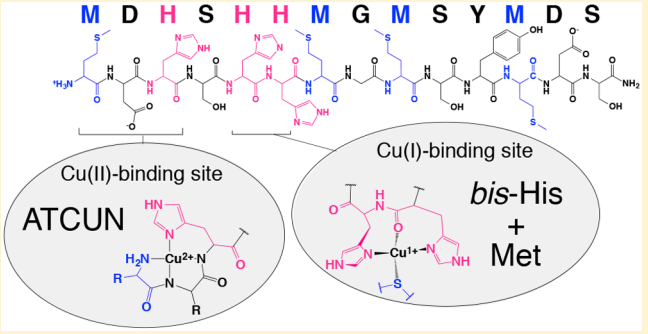

Cellular and systemic copper acquisition and trafficking are essential to eukaryotic life. In mammals, Cu is required for the function of essential enzymes, including copper−zinc superoxide dismutase, cytochrome-*c* oxidase, lysyl oxidase, ceruloplasmin, dopamine β-hydroxylase, tyrosinase, peptidyl-glycine monooxygenase, clotting factors V and VIII, angiogenin, hephaestin, and others.[1,2] Cells acquire Cu from the extracellular environment primarily through the plasma membrane copper transporter (Ctr1).[3−6] Mammalian Ctr1 is essential for embryogenesis,[7,8] the mitogen-activated protein (MAP) kinase pathway,[9] neuronal development and signaling,[10,11] and immunity.[12] In addition, Ctr1 involvement is implicated in development of platinum-drug resistance in certain human cancers[13] and in human neurodegenerative disorders[14−17] including Parkinson's[18,19] and Alzheimer's diseases.[20−22] The critical nature of Ctr1 in human health has spurred interest in, and investigation of, Ctr1 structure and function; however, the molecular details of Ctr1-dependent Cu transport are only beginning to be understood.

Functional Ctr1 homotrimerizes in the plasma membrane forming cone-shaped pores that specifically transport Cu(I). Monomeric human Ctr1 is a 190 amino acid protein with three transmembrane domains, an intracellular loop (47 amino acids), one short intracellular C-terminal domain (15 amino acids), and a longer extracellular N-terminal domain (67 amino acids).[23−29] The extracellular N-terminal domain of human Ctr1 is largely unstructured, rich in histidine (His) and methionine (Met) Cu-binding motifs, and responsible for Cu acquisition from extracellular Cu carriers.[30−32]

Ctr1 proteins of metazoan species contain conserved Met-rich and His-rich clusters in their unstructured[23,24,26,33] N-terminal domain (Table 1). Mammalian cell culture studies of Ctr1 have shown that conserved Met and His motifs are important for high-affinity copper acquisition under copper-limiting conditions.[30,34] The HH (*bis*-His) sequence in human Ctr1 has also been implicated in serving a reductase-like role in the presence of ascorbic acid. As such it has analogies to the amyloid-β (Aβ) peptide of Alzheimer's disease, which stabilizes Cu(I) within a linear *bis*-His coordination environment.[35−38] Although an understanding of Cu(I)−Ctr1 is interesting and could shed light on the mechanism of Ctr1-dependent Cu reduction and transport, no experimental data has been

Received: May 29, 2015
Published: August 10, 2015

DOI: 10.1021/acs.inorgchem.5b01162
Inorg. Chem. 2015, 54, 8544−8551

Table 1. Multiple Sequence Alignment for the Ctr1 N-Terminal Domain (residues 1−25 shown, human numbering) from Representative Species[a]

Human	MD**H**---S**H**-----**H**MGMS-YMD----S-N-ST-MQPS-**HHH**P
Chimpanzee	MD**H**---S**H**-----**H**MGMS-YMD----S-N-ST-MQPS-**HHH**P
Boar	MD**H**---SA-----**H**MGMST**H**MGMS--DMN**H**STTM-PPS**HHH**P
Mouse	MN**H**MGMN**H**MEM**HHH**MGMN-**H**TD----D-N-IT-M-PP-**HHH**P
Cow	MG**H**---S**H**-----IMGMN--MDMSGGD-N-ST-M-PP-**HHH**P

[a]Full-N-terminal Ctr1 alignments shown in Supporting Information.

published on the coordination structure of Cu(I)−Ctr1 protein or model peptides until now.

Recent evidence suggests that human serum albumin can directly interact with a model peptide of the Ctr1 N-terminal (designated Ctr1−14: MDHSHHMGMSYMDS),[39] and further evidence demonstrates that serum albumin can transfer Cu(II) to the extracellular domain of Ctr1.[40] Because Ctr1 specifically transports Cu(I) across the plasma membrane, extracellular Cu(II) must therefore be reduced to Cu(I) prior to Ctr1-dependent transport. The six-transmembrane epithelial antigen of prostate (STEAP) proteins may additionally serve as an auxiliary copper reductase in mammals;[41−44] however, evidence for the functional significance of STEAP proteins in Ctr1-dependent Cu transport is lacking. On the other hand, the rate of transport and total cellular copper load increases significantly in the presence of the biological reductant, ascorbic acid (Vitamin C).[29,45] Evidence from studies on the Ctr1−14 peptide demonstrate that the N-terminal sequence of Ctr1 may be capable of facilitating ascorbate-dependent reduction of Cu(II) by virtue of its specific sequence of His residues.[30] If Ctr1 can facilitate ascorbate-dependent Cu(II) reduction then copper reductase proteins may not be required for Ctr1-dependent Cu transport under certain biological conditions. The His-rich motifs of interest in the Ctr1−14 peptide include the N-terminal NH_2-XXH (amino terminal high affinity Cu(II) and Ni(II) or "ATCUN")[46−48] Cu(II) binding site (log $K_{Cu(II)}$ = 11.0) and an adjacent *bis*-His (HH) sequence that may recruit participation of a nearby methionine (Met) in the peptide's high-affinity Cu(I) binding site (log $K_{Cu(I)}$ = 12.8).[30]

The Ctr1−14 peptide is unique to typical ATCUN-type peptides in that it facilitates the reduction of Cu(II) bound in its ATCUN site.[49] The interesting ability of Ctr1−14 model peptide to facilitate ascorbate-dependent Cu(II) reduction requires the presence of a *bis*-His site, which appears at positions 5 and 6 in the native sequence of human Ctr1 (Table 1).[30] It is likely that the Cu coordination environments provided by Ctr1−14 define the redox behavior of Cu bound to this peptide. The Cu(II) binding site is a 4-N square planar environment typical of ATCUN-type peptides. However, the specific identity and coordination geometry of the Cu(I) site has not been elucidated from previous work. Here, we use insight from NMR, XAS, and molecular modeling to shed light on the identity of the Cu(I) binding site of the Ctr1−14 model peptide.

EXPERIMENTAL SECTION

Peptide Synthesis and Purification. Model peptide based on the first 14 amino acids of the extracellular N-terminal domain of Ctr1 (Ctr1−14: MDHSHHMGMSYMDS) and a series of mutants where individual methionines (Met, M) were substituted for the non-coordinating amino acid, norleucine (Nle) (M1Nle, NleDHSHHMGMSYMDS; M7Nle, MDHSHHNleGMSYMDS; M9Nle, MDHSHHMGNleSYMDS; M12Nle, MDHSHHMGMSYNleDS) were synthesized on a Protein Technologies PS3 automated peptide synthesizer on Rink Amide MBHA Low Loaded Resin (Protein Technologies) on a 0.2 mmol scale. Couplings of standard 9-fluoromethoxy-carbonyl (Fmoc)-protected amino acids (Chem-Impex) were achieved using HCTU (*O*-(6-chlorobenzotriazol-1-yl)-*N*,*N*,*N*′,*N*′-tetramethyluronium hexafluorophosphate, Protein Technologies) in the presence of NMM (*N*-methylmorpholine, Sigma-Aldrich) in DMF (*N*,*N*′-dimethylformamide, Protein Technologies) for 10 min cycles. Fmoc deprotection was achieved with 20% piperidine in DMF. The N-terminus was left as the free amine. Side chain deprotection and peptide cleavage from the resin were achieved by treating the resin-bound peptide with 7−10 mL of a cocktail of 95% trifluoroacetic acid (TFA), 2.5% ethane dithiol (EDT), and 2.5% triisopropylsilane (TIS, Sigma-Aldrich) for 4 h under N_2. An additional 150 μL of EDT and 130 μL of bromotrimethylsilane (TMSBr, Sigma-Aldrich) were added during the last 30 min to minimize methionine oxidation and to scavenge carbocations. A stream of N_2 was used to evaporate TFA to a volume of ∼2 mL. Peptides were precipitated and washed 3 times with 10 mL of diethyl ether (Sigma-Aldrich). Peptides were air dried and then purified by preparatory reverse-phase HPLC on a YMC C18 Column with a linear gradient from 7% to 97% acetonitrile in water with 0.1% TFA. Purity was validated to >95% by analytical HPLC, and the mass of the peptide was confirmed by ESI-MS. Ctr1−14 peptide calculated m/z where z = 2 (Peptide + $2H^+$) 818.23. Found: (Peptide + $2H^+$) 818.49.

Preparation of Stock Solutions. Stock solutions of peptides were made by dissolving lyopholyzed peptide in 1 mL of Nanopure water. Concentration was determined using the Edelhoch method.[50] In short, 5−10 μL of peptide stock was diluted in 1 mL of Nanopure water to get a UV absorbance between 0.1 and 1 absorbance unit at 280 nm. Absorbance of amino acid side chains, in this case, only tyrosine, at 276, 278, 280, and 282 nm was measured, and total concentration of peptide was determined using known extinction coefficients of tyrosine at these wavelengths.[50] Peptide stock solution was stored in sealed containers in a N_2 environment. Cu(I) stock solutions were prepared fresh daily by dissolving tetrakisacetonirile Cu(I) hexafluorophsophate ($[Cu(CH_3CN)_4]PF_6$, Sigma-Aldrich) in anhydrous acetonitrile (Sigma-Aldrich) under a N_2 atmosphere using a Coy anaerobic chamber. Cu(I) stock solutions were standardized by titrating aliquots of stock solution into an excess of the chromophoric ligand anion bicinchoninate (BCA, Sigma) in degassed, Nanopure water. Concentration was determined from absorption of the Cu(I) $(BCA)_2$ complex (λ_{max} = 562 nm, ε = 7900 M^{-1}).[51]

NMR Spectroscopy. Samples of peptide in phosphate buffer were prepared in water and then twice lyophilized and redissolved in degassed D_2O. Cu(I) was added to samples under anaerobic conditions. Final concentrations of a series of samples with serial increase in [Cu(I)] were 10 mM phosphate buffer (pH 7.4) and 0.25 mM Ctr1−14 peptide with 0, 0.0625, 0.125, 0.1875, or 0.25 mM Cu(I) (4 sample conditions with Cu:P ratios of 0, 0.25, 0.5 0.75, or 1). Samples were placed in separate quartz NMR tubes under N_2 atmosphere and sealed with septa. ^{1}H NMR spectra were taken with a 600 MHz Varian NMR and a controlled-temperature probe at 30 °C (Duke University), and Cu(I)−peptide binding was monitored by observing changes in ^{1}H chemical shifts with increasing Cu:peptide ratios. Water suppression was achieved using the PRESAT pulse sequence.

DOI: 10.1021/acs.inorgchem.5b01162
Inorg. Chem. 2015, 54, 8544−8551

Cu K-Edge X-ray Absorption Spectroscopy. Solutions of Cu(I) with Ctr1−14 (1 mM peptide, 0.8 mM $[Cu(I)(CH_3CN)_4]PF_4$; 20 mM HEPES, 50% v/v glycerol) were prepared under an N_2 atmosphere, injected into VeroWhite sample holders with a Mylar tape window, and rapidly frozen. HEPES buffer was chosen for its temperature-stable pH buffering capacity.[52,53] Although HEPES is known to weakly coordinate Cu(II)[54] and to participate in Cu(II) reduction in some cases,[55] there is no evidence that HEPES coordinates Cu(I). Steric bulk interferes with HEPES coordination to metal ions,[54] and with the bulky peptide ligand studied here, ternary HEPES complexes are further unlikely. Inspection of the samples prior to data collection indicated the frozen solutions were glasses with no obvious ice crystals within the samples.

Data was collected at the Stanford Synchrotron Radiation Lightsource (SSRL), with the SPEAR storage ring containing 500 mA and operating at 3.0 GeV, using the XAS Collect[56] data acquisition software. Cu K-edge data were collected on the structural molecular biology XAS beamline 7-3, employing a Si(220) double-crystal monochromator. Beamline 7-3 employs a Rh-coated vertically collimating mirror upstream of the monochromator, with harmonic rejection achieved by setting the mirror cutoff angle to 12 keV. Incident and transmitted X-ray intensities were monitored using N_2-filled ionization chambers, with a sweeping voltage of 1800 V. X-ray absorption was measured as the Cu Kα fluorescence excitation spectrum using a Ge array detector (Canberra Ltd. Meriden, CT, USA).[57] During data collection the sample was maintained at 10 K using an Oxford Instruments liquid He flow cryostat. A total of 14 spectra were accumulated with a k range of 15.75 $Å^{-1}$. The energy of the incident beam was calibrated by reference to the absorption of a Cu foil measured simultaneously with each fluorescence spectrum, with the lowest energy inflection point calibrated to 8980.3 eV. The energy threshold (E_0) for Cu EXAFS oscillations was assumed to be 9000 eV.

EXAFS Data Analysis. The EXAFS oscillations $\chi(k)$ were quantitatively analyzed by curve fitting using EXAFSPAK,[58] as previously described,[59] using ab initio theoretical phase and amplitude functions from the program FEFF, version 8.25.[60,61] No additional smoothing, filtering, or related operations were performed on the data. Multiple scattering models used in the fitting procedure were obtained from geometry-optimized DFT models of Cu(I) bound to various fragments of the Ctr1 N-terminal region (see computational section below).

Density Functional Structure Calculations. Density functional structure calculations were carried out with the Gaussian09, revision D.01, quantum chemistry package.[62] Closed shell Cu(I) complexes were optimized without geometry or symmetry constraints using the B3LYP hybrid functional method with the 6-311+G(2df,2p) basis set. Structures were considered optimized when the change in energy between subsequent optimization steps fell below 0.05 J mol^{-1}. To ensure optimized structures represented stationary points on the potential energy surface harmonic frequency calculations were calculated at the same level of theory as geometry optimizations. The stabilizing effect of bulk solvation on the gas-phase-optimized structures was modeled using the integral equation formalism variant of the polarizable continuum model, IEFPCM,[63] with united atom radii defining the molecular cavity and a dielectric representing water (ε = 78.39), calculated at the same level of theory as above. Calculated free energy comparisons were made following previously described methods.[64]

RESULTS AND DISCUSSION

Results from a recent study by Haas and Franz showed that the Ctr1−14 model peptide coordinates Cu(II) with 10 pM affinity and Cu(I) with 0.2 pM affinity in aqueous solution buffered at pH 7.[30] Serial substitution of Cu(I)-binding amino acids in model peptides revealed that both His and Met residues were required to maintain picomolar binding affinity. This previous work also revealed interesting redox chemistry of Cu(II)−Ctr1−14 model peptides with ascorbic acid. The Ctr1−14 model peptide contains an ATCUN site; however, unlike typical ATCUN peptides, Cu(II) bound to this site is easily reduced by a near-equimolar amount of ascorbic acid. This apparent facilitation of Cu(II) reduction was observed only in Ctr1 model peptides that contained the intact native HH (*bis*-His) site in the 5−6 positions from the N-terminus (Table 1). The identity of the Cu(I) binding site, however, was not determined. Here, we aimed to characterize the Cu(I) binding site of the N-terminal region of Ctr1 in order to gain structural insight into the previously observed redox properties of the Ctr1−14 peptide as well as the initial events in the mechanism of Cu transport via Ctr1.

As Ctr1 is a transport protein we hypothesized that the protein would facilitate Cu(II) reduction, by providing a favorable Cu(I) binding site, and also bind Cu(I) in such a manner as to allow quick exchange of ligands for subsequent Cu(I) transfer toward the cytoplasm following reduction. Here we demonstrate that the Cu(I)-binding environment of Ctr1−14 is best described as a 4-coordinate site, which includes a *bis*-His, one methionine, and a carbonyl oxygen from the protein backbone. This site is consistent with the mixed Met and His site proposed based on previously published data[30] and satisfies the predicted characteristics of a redox-active[35] and highly labile Cu(I) site, ideal for the role of Ctr1 in facilitating the initial reduction of Cu(II) and subsequent transport of Cu(I) across the plasma membrane.

Structure Calculations. DFT calculations of the aqueous free energies for stepwise coordination of Cu(I) with model ligands of His (4-methylimidazole, MeIm), Met (dimethylsulfide, SMe_2), and 2-His model peptides (Ac-HSH-NH_2 and Ac-HH-NH_2) starting from aquo−Cu(I) complex) indicated that two-coordinate Cu(I) is generally more stable than 3- or 4-coordinate modes. Compared to $[Cu(OH_2)_2]^+$, replacement of both water molecules with imidazole yields the most favorable coordination mode;[62] however, as will be discussed below, there may be additional considerations which give rise to alternate variations of this core coordination geometry.

In order to obtain reasonable starting structural models for comparison with EXAFS data, small model peptides of the Ctr1−14 sequence were modeled to account for geometric constraints imposed by the peptide backbone (Ac-HSH-NH_2 and Ac-HH-NH_2). From these model peptide calculations, we identified stable 2-N(imidazole) coordination geometries for both the HSH sequence as well as the HH sequence. From these calculations we observe O-atom coordination from backbone carbonyls in both the HSH and the HH models, corresponding to N_2O_2 and N_2O coordination environments, respectively (see Figure S8 in Supporting Information). In both model systems the additional donor atom recruitment to the Cu(I) center is due to the constraints imposed on the local peptide backbone upon Cu coordination to the His side chains, which in turn distorts the coordination geometry of the His side chains away from the preferred linear 2-coordinate arrangement.

NMR Data. Hard−soft acid−base (HSAB) theory predicts that borderline His-N and soft Met-S donors of Ctr1−14 peptide are best suited for bonding to the soft Cu(I) ion. Aromatic and methyl ^1H NMR chemical shifts of His and Met, respectively, are conveniently separated from backbone amide and most other side chain ^1H shifts, and changes in these chemical shifts are observed upon metal-ion coordination.[31] The full ^1H NMR spectrum of Ctr1−14 peptide in D_2O appears in Figure 1, with inset plots highlighting regions of

DOI: 10.1021/acs.inorgchem.5b01162
Inorg. Chem. 2015, 54, 8544−8551

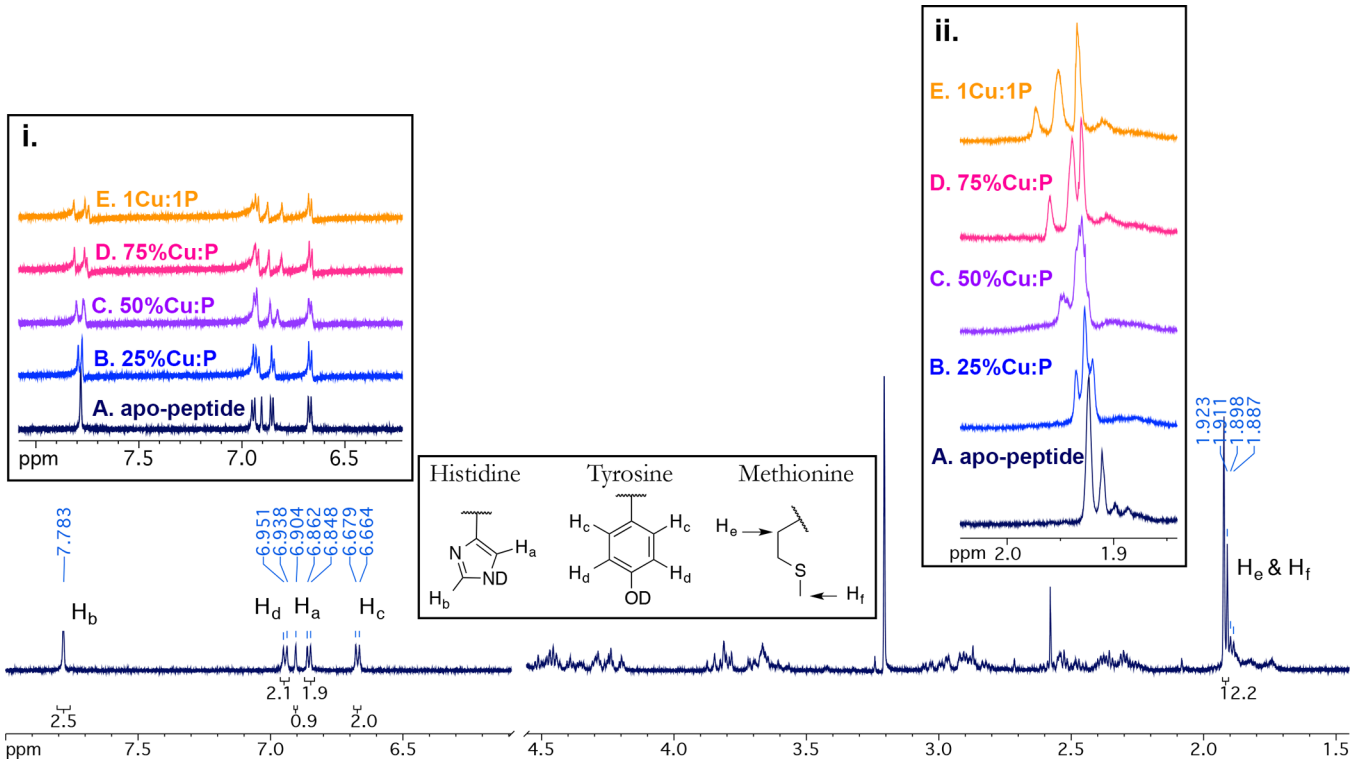

Figure 1. ^{1}H NMR spectrum of Ctr1−14 peptide and changes in the NMR spectrum as Cu(I):peptide ratio increases (inset i and ii). Signals from aromatic ^{1}H from His and Tyr are shown magnified in inset i, and signals from methyl and methylene ^{1}H from Met are shown magnified in inset ii. Changes in His and Met chemical shifts are apparent upon addition of Cu(I), while those of noncoordinating Tyr do not shift upon Cu(I) addition (see SI). This data indicates that specific His and Met residues exclusively interact with Cu(I).

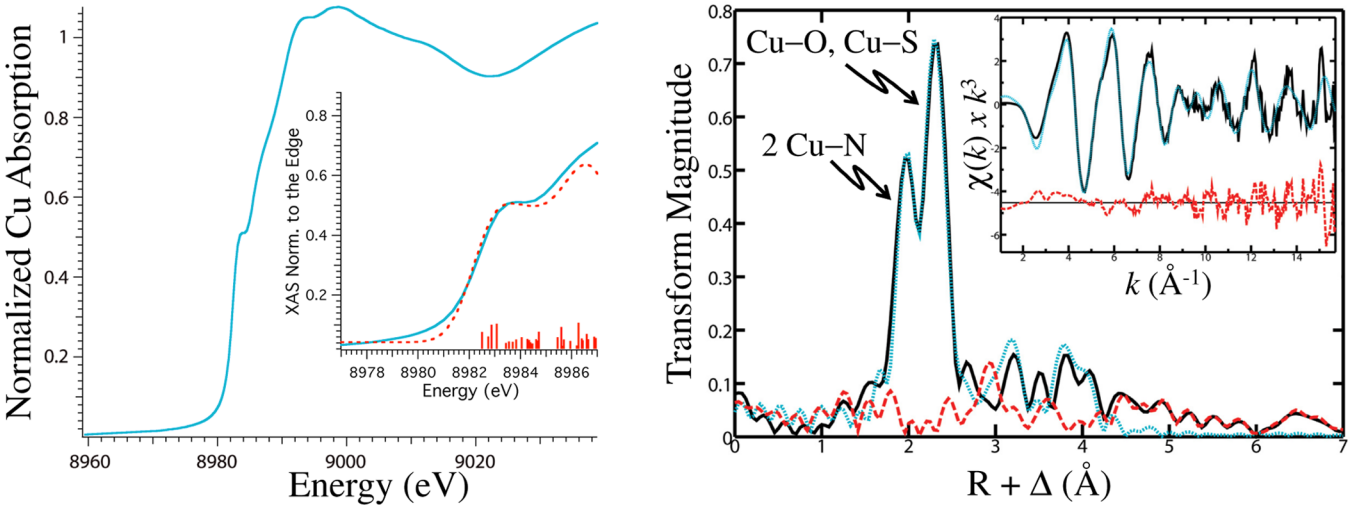

Figure 2. Cu K-edge near-edge spectrum (left) confirms that the copper bound to Ctr1−14 is Cu(I). Inset depicts the TD-DFT simulation to the pre-edge feature using the four-coordinate computational model [Cu^{I}(Ac-HH-NH$_2$)(S(CH$_3$)$_2$)] (shown in Figure 3). Experimental data are shown in blue, simulation is shown as the red dashed line, and 50 lowest energy bound transitions are given as red sticks. (Right) EXAFS curve-fitting results with multiple scattering using a 4-coordinate Cu(I) complex, comprised of two imidazole donors as well as longer distance Cu−O and Cu−S backscatterers (generated from the model shown in Figure 3). In the EXAFS and EXAFS Fourier transform plots the solid black line corresponds to the experimental data, the dotted blue line is the best fit to the experimental data, and the red line is the residual.

interest as Cu(I) is increased relative to peptide. Assignments of His, Tyr, and Met H atoms are indicated. In the apo-peptide, His and Tyr aromatic ^{1}H signals appear between 6.5 and 8 ppm (Figure 1, inset i). The four aromatic ^{1}H peaks arising from Tyr are observed as two 2-H doublets just below 7 ppm. His aromatic ^{1}H peaks usually appear as two singlets between 6.5 and 8.5 and are highly sensitive to pH changes close to neutral. In the aromatic region of the apo-Ctr1−14 ^{1}H NMR spectrum (Figure 1, inset i, spectrum a) the H_a and H_b signals of the His imidazole moiety are distinctly resolved. We observe one singlet from each of the three His H_b protons overlapping at approximately 7.8 ppm, appearing as one singlet. Three H_a peaks are slightly separated, appearing as three individual singlets from 6.8 to 6.9 ppm. These Histidine H_a and H_b peaks

DOI: 10.1021/acs.inorgchem.5b01162
Inorg. Chem. 2015, 54, 8544−8551

further separate upon increasing concentration of Cu(I), indicating that the His residues are coordinating to Cu(I). The Tyr signals did not shift with increasing concentration of Cu(I). Methyl (CH_3) and methylene (CH_2) moieties from the four methionine residues present in the Ctr1 sequence of the metal-free peptide appear as overlapping peaks just below 2 ppm in the apo-peptide spectrum (Figure 1, inset ii, spectrum a). Two singlet peaks at 1.923 and 1.911 can account for 12 methyl protons from four Met residues (integrate as 12 total H). These peaks separate and shift upfield as the Cu(I):peptide ratio is increased, indicating that the environment of these methyl groups is becoming deshielded. This observation is consistent with Met coordination to Cu(I) in this peptide. No significant changes in noncoordinating Tyr side chain ^{1}H chemical shifts were observed during the course of the Cu(I) titration (Figure 1, inset i, see also SI, Table S1). This NMR data is consistent with the assignment of a mixed Met and His Cu(I) coordination site, as previously proposed from model peptide solution competition studies.[30]

X-ray Absorption Spectroscopy Data. Cu K-edge X-ray absorption spectroscopy (Figure 2) was utilized to gain insight into the coordination geometry and ligand environment about the Cu(I) center.

Initial curve fitting of the experimental EXAFS spectrum was best modeled as a 4-coordinate Cu(I) center, with two Cu−N/O backscattering atoms at 2.02 Å, one Cu−N/O at 2.19 Å, and one Cu−S at 2.31 Å. The theoretical resolution, ΔR, based on a k range of 1−15.7 Å^{-1}, is 0.11 Å, which is sufficiently below the separation between the first two shells of light atom backscatterers that the fit result is expected to be reliable. Moreover, the light atom backscatterer at 2.19 Å and the Cu−S backscatterer mutually cancel a significant portion of their contribution from the spectrum, such that without the long backscattering atom at 2.19 Å the fit is significantly diminished. Attempts to fit the data without a Cu−S backscattering component yielded the poorest fits, while omitting the Cu−S phase in favor of a light atom (such as N or O) distorts the peak shapes in the Fourier transform and gives rise to a slight broadening, indicating that a heavier atom like S is required for correctly modeling the EXAFS oscillations as well as correctly phasing the data. Visual inspection of the EXAFS Fourier transform, between ∼3 and 4.5 Å, indicated the involvement of coordination by imidazole from one or more histidines. In order to model this type of interaction we resorted to a full multiple scattering model in order to better represent the data.

The DFT geometry-optimized structure shown in Figure 3 was used to generate the multiple scattering model, which included heavy atoms within 5 Å of the Cu center. This model generated 36 unique scattering paths, from which each of the individual coordinating Cu−N paths were combined into a single scattering path with $N = 2$. The multiple scattering model was in full agreement with the results obtained from the single scattering approximation, with 2 Cu−N at 2.02 Å, 1 Cu−O at 2.19 Å, and 1 Cu−S at 3.31 Å. The complete results of the EXAFS curve fitting are summarized in Table S4.

A Cambridge Structure Database (CSD)[65,66] search for similar Cu(I) complexes reveals that the DFT structures tended toward shorter Cu−N(imidazole) bond lengths overall, while the Cu−N backscattering distances from the EXAFS curve fitting were generally in agreement with the bond lengths observed in the structurally similar Cu(I) structure reported by Wang et al.[67]

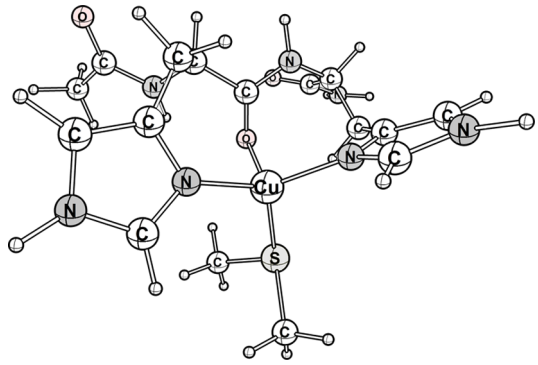

Figure 3. DFT geometry-optimized structure of [Cu^I(Ac-HH-NH_2)($S(CH_3)_2$)] model complex, which afforded the best fit to the EXAFS data and reproduces the XANES edge structure by TD-DFT methods.

To specifically identify the coordinating methionine observed for the native Cu(I)−Ctr1−14 structure, experimental XAS data was collected on a series of "mutant" peptides where each methionine was individually substituted for the noncoordinating, but structurally similar, norleucine (Nle) residue. All of the Met → Nle mutant peptides give slightly distorted Cu(I) complexes, as judged by XAS spectroscopy, compared to the native Ctr1−14 sequence (see near-edge spectra in Supporting Information Figure S7). The Cu(I) complexes of M1Nle, M7Nle, and M9Nle peptides appear to be the most structurally dissimilar to the native Cu(I)−Ctr1−14, preferring one long Cu−S backscattering donor and two additional light atom Cu−N/O donors at an equivalent bond length. We conclude that the two Cu−N/O donors of the M1Nle, M7Nle, and M9Nle peptides are two His imidazole donors based on multiple scattering fits to the EXAFS. Only the EXAFS spectrum of Cu(I)−M12Nle could be fit to the multiple scattering model employed in the wild-type Ctr1−14 fit (Table S4), albeit with subtly altered fit parameters, including 2 Cu−N at 1.99 Å, 1 Cu−O at 2.18 Å, and 1 Cu−S at 2.27 Å. From the Met → Nle XAS data we conclude that the one Met S-donor atom used to fit the Cu(I)−Ctr1−14 EXAFS data is likely a combination of contributions from M1, M7, and M9 of the Ctr1−14 sequence. The Met ligand, therefore, appears to be labile and exchangeable among these three side chains (see Supporting Information), as disruption of any one of them subtly alters the Cu(I) coordination. Alternatively, one or more of these Met residues may also play a role in tertiary structural interactions that are required to create the native-sequence Cu(I)−Ctr1−14 structure.

For Cu(I)−Ctr1, the identity of the longer light atom scatterer as an oxygen donor is based on the DFT structure calculations. Further support for the proposed structure was obtained based on an analysis of the pre-edge features of the Cu K-edge spectrum of Cu(I)− Ctr1 (see Supporting Information). The pre-edge region shows a shoulder feature at 8983.5(1) eV that is buried into the edge. The appearance of the edge is therefore consistent with 4-coordinate Cu(I) in a tetrahedral coordination environment.[68] We propose that this long Cu−O bond is derived from a carbonyl oxygen from the peptide backbone. The EXAFS curve-fitting parameters for the native Ctr1 peptide are therefore in good agreement with the [Cu^I(Ac-HH-NH_2)($S(CH_3)_2$)] structure (Figure 3), with two Cu− $N_{imidazole}$ at 1.95 Å, Cu−S at 2.35 Å, and Cu−O at 2.16 Å.

DOI: 10.1021/acs.inorgchem.5b01162
Inorg. Chem. 2015, 54, 8544−8551

To gain a deeper understanding of the coordination geometry about the Cu(I) center we modeled the edge features of the X-ray absorption spectrum. Using TD-DFT methods (B3LYP/def2-tzvp(-f)) a series of Cu K-edge spectra was simulated in different two-, three-, and four-coordinate environments (Figure S6 in Supporting Information). An excellent fit to the experimental edge (Figure 2) was obtained with a computational model containing Cu(I) in a *bis*-His coordination environment with the two histidine ligands in a trans coordination environment, a carbonyl oxygen from the amide between the coordinating His residues, and a S-based thioether ligand ($[Cu^{I}(Ac\text{-}HH\text{-}NH_2)(S(CH_3)_2]^+$, Figure 3).

On the basis of the Cu K-edge XAS data we propose that the Cu(I) center in Ctr1 is contained in a quasi 4-coordinate distorted tetrahedral N_2OS coordination environment. The identity of the nitrogen- and oxygen-based ligands are likely derived from the H(5)H(6) moiety, with the nitrogen atoms derived from the imidazole groups of H(5) and H(6). These imidazole ligands are found in a trans-like orientation. We also propose that the carbonyl group comprising the H(5)H(6) amide bond provides the long oxygen-based ligand to Cu(I). This is a similar Cu(I) coordination environment as found in the Cu(I) complex of the Aβ peptide and a prion protein (PrP) model system, both of which display a trans imidazole coordination motif about Cu(I).[35−38,64] However, unlike these examples, the *bis*-His moiety about the Cu(I) center of Cu(I)−Ctr1 was found to be significantly distorted away from linearity and contained an additional thioether-based ligand from an unidentified methionine thioether group. It is worth noting that neither Aβ peptide nor the prion model peptide possesses a methionine in close proximity to the Cu(I) coordination site. The close proximity of a number of viable methionine-based ligands to the H(5)H(6) moiety in Ctr1 may be responsible for the deviations in the Cu(I) coordination environment of Cu(I)−Ctr1 vs Cu(I)−Aβ and Cu(I)−PrP.

Conclusions and Biological Significance. The data presented here for the Cu(I)−Ctr1−14 complex are consistent with a quasi-tetrahedral 4-coordinate 2N(His)-1S(Met)-1O-(backbone) coordination and closely match the modeled binding site in Figure 3, containing two imidazole nitrogens from *bis*-His (His 5 and 6), a backbone carbonyl oxygen from His5, and one Met sulfur. This 4-coordinate site is less stable and therefore likely to be more labile than *bis*-His or other 2-coordinate-type Cu(I) sites. The identity of this labile Cu(I) binding site can be used to rationalize the mechanism by which Cu(I) reduction is facilitated by this model peptide and is consistent with the expected lability required for effective Cu(I) transport. Maintaining Cu(I) in a labile coordination environment is energetically advantageous and a necessity for transport in this system. On the basis of this and previous studies[30,39,40] we envision a model for copper transport where Cu(II) may be directly transferred to Ctr1 by HSA or other Cu carriers in the extracellular environment. Once bound at the N-terminus of Ctr1, Cu(II) is reduced in the presence of biological reductant, such as ascorbate, as observed in Cu-Aβ.[37,38] Considering the thermodynamic stability of Cu(I) coordinated in a linear *bis*-His motif over the Cu(II) oxidation state,[69] the two adjacent His residues may be vital in driving the reduction of Cu(II) to Cu(I) despite the ATCUN-type Cu(II) coordination environment.

Once reduced, copper could then be shuttled through a series of labile Cu(I) sites, beginning with the pseudotetrahedral Cu(I) site characterized here for the Ctr1−14 peptide. The pseudotetrahedral coordination environment may therefore be vital in copper transport. Linear Cu(I) is known to be thermodynamically stable and does not readily undergo ligand substitution reactions. Coordination of Cu(I) in a pseudotetrahedral environment may yield a Cu(I) coordination complex that will more readily undergo ligand exchange. Cu(I) may then be exchanged through a series of labile sites down a concentration gradient and/or a thermodynamic stability gradient, until it reaches the cytoplasm and is ultimately transferred to intracellular Cu chaperones. Future studies are aimed at probing this supposition.

■ ASSOCIATED CONTENT

Supporting Information

The Supporting Information is available free of charge on the ACS Publications website at DOI: 10.1021/acs.inorgchem.5b01162.

Metazoan full Ctr1 multiple sequence alignment, full ^{1}H NMR spectra and chemical shifts, experimental XAS data on Cu(I)−Ctr1 from NSL, plots of the Cu K-edge pre-edge features for a series of computational model compounds generated by TD-DFT methods, experimental XAS data on Cu(I)−Met → Nle mutant peptides, Cartesian coordinates for modeled coordination structures, and alternative fits to the EXAFS data (PDF)

■ AUTHOR INFORMATION

Corresponding Author

*E-mail: khaas@saintmarys.edu. Phone 574-284-4660.

Author Contributions

The manuscript was written by K.L.H. through contributions of all authors. M.J.P., K.S., and J.S. contributed data, and K.J.F. contributed critical resources. All authors contributed to discussion and editing. All authors have given approval to the final version of the manuscript.

Notes

The authors declare no competing financial interest.

■ ACKNOWLEDGMENTS

K.L.H. acknowledges financial support from the Lilly Endowment, Saint Mary's College, Department of Chemistry & Physics, the Center for Academic Innovations at Saint Mary's College, and a Maryjean R. Burke and Daughters SISTAR award. J.S. acknowledges financial support from the National Science Foundation (CHE-1362662). Portions of this research were carried out at the Stanford Synchrotron Radiation Lightsource, a Directorate of SLAC National Accelerator Laboratory and an Office of Science User Facility operated for the U.S. Department of Energy Office of Science by Stanford University. The SSRL Structural Molecular Biology Program is supported by the DOE Office of Biological and Environmental Research, and by the National Institutes of Health, National Center for Research Resources, Biomedical Technology Program (P41RR001209). Use of the National Synchrotron Light Source, Brookhaven National Laboratory, was supported by the U.S. Department of Energy, Office of Science, Office of Basic Energy Sciences, under Contract No. DE-AC02-98CH10886. Cu K-edge studies were preformed on beamline X3-b, which is supported through the Case Center for Synchrotron Biosciences, which is funded through the National Institute of Biomedical Imaging and Bioengineering (NIH

DOI: 10.1021/acs.inorgchem.5b01162
Inorg. Chem. 2015, 54, 8544−8551

grant no. P30-EB-009998). Portions of this research were enabled by support provided by WestGrid (www.westgrid.ca) and Compute Canada Calcul Canada (www.computecanada.ca). K.L.H., K.J.F., and M.J.P. acknowledge CanBIC 2013 for germination of this collaborative work.

REFERENCES

(1) Festa, R. A.; Thiele, D. J. *Curr. Biol.* **2011**, *21*, R877−R883.
(2) Pena, M. M. O.; Lee, J.; Thiele, D. J. *J. Nutr.* **1999**, *129*, 1251−1260.
(3) Maryon, E. B.; Molloy, S. A.; Zimnicka, A. M.; Kaplan, J. H. *BioMetals* **2007**, *20*, 355−364.
(4) Turski, M. L.; Thiele, D. J. *J. Biol. Chem.* **2009**, *284*, 717−721.
(5) Ohrvik, H.; Thiele, D. J. *Ann. N. Y. Acad. Sci.* **2014**, *1314*, 32−41.
(6) Kim, B. E.; Nevitt, T.; Thiele, D. J. *Nat. Chem. Biol.* **2008**, *4*, 176−185.
(7) Lee, L. W.; Prohaska, J. R.; Thiele, D. J. *Proc. Natl. Acad. Sci. U. S. A.* **2001**, *98*, 6842−6847.
(8) Kuo, Y. M.; Zhou, B.; Cosco, D.; Gitschier, J. *Proc. Natl. Acad. Sci. U. S. A.* **2001**, *98*, 6836−6841.
(9) Turski, M. L.; Brady, D. C.; Kim, H. J.; Kim, B. E.; Nose, Y.; Counter, C. M.; Winge, D. R.; Thiele, D. J. *Mol. Cell. Biol.* **2012**, *32*, 1284−1295.
(10) Dodani, S. C.; Firl, A.; Chan, J.; Nam, C. I.; Aron, A. T.; Onak, C. S.; Ramos-Torres, K. M.; Paek, J.; Webster, C. M.; Feller, M. B.; Chang, C. J. *Proc. Natl. Acad. Sci. U. S. A.* **2014**, *111*, 16280−16285.
(11) Dodani, S. C.; Domaille, D. W.; Nam, C. I.; Miller, E. W.; Finney, L. A.; Vogt, S.; Chang, C. J. *Proc. Natl. Acad. Sci. U. S. A.* **2011**, *108*, 5980−5985.
(12) Hodgkinson, V.; Petris, M. J. *J. Biol. Chem.* **2012**, *287*, 13549−13555.
(13) Arnesano, F.; Losacco, M.; Natile, G. *Eur. J. Inorg. Chem.* **2013**, *2013*, 2701−2711.
(14) Nevitt, T.; Ohrvik, H.; Thiele, D. J. *Biochim. Biophys. Acta, Mol. Cell Res.* **2012**, *1823*, 1580−1593.
(15) Waggoner, D. J.; Bartnikas, T. B.; Gitlin, J. D. *Neurobiol. Dis.* **1999**, *6*, 221−230.
(16) Hordyjewska, A.; Popiolek, L.; Kocot, J. *BioMetals* **2014**, *27*, 611−621.
(17) Faller, P.; Hureau, C.; La Penna, G. *Acc. Chem. Res.* **2014**, *47*, 2252−2259.
(18) Montes, S.; Rivera-Mancia, S.; Diaz-Ruiz, A.; Tristan-Lopez, L.; Rios, C. *Oxid. Med. Cell. Longevity* **2014**, *2014*, Article ID 147251, 15 pages.10.1155/2014/147251
(19) Davies, K. M.; Bohic, S.; Carmona, A.; Ortega, R.; Cottam, V.; Hare, D. J.; Finberg, J. P. M.; Reyes, S.; Halliday, G. M.; Mercer, J. F. B.; Double, K. L. *Neurobiol. Aging* **2014**, *35*, 858−866.
(20) Lang, M. L.; Fan, Q. W.; Wang, L.; Zheng, Y. J.; Xiao, G. R.; Wang, X. X.; Wang, W.; Zhong, Y.; Zhou, B. *Neurobiol. Aging* **2013**, *34*, 2604−2612.
(21) Zheng, Z. Q.; White, C.; Lee, J.; Peterson, T. S.; Bush, A. I.; Sun, G. Y.; Weisman, G. A.; Petris, M. J. *J. Neurochem.* **2010**, *114*, 1630−1638.
(22) Opazo, C. M.; Greenough, M. A.; Bush, A. I. *Front. Aging Neurosci.* **2014**, *6*, 7.
(23) Tsigelny, I. F.; Sharikov, Y.; Greenberg, J. P.; Miller, M. A.; Kouznetsova, V. L.; Larson, C. A.; Howell, S. B. *Cell Biochem. Biophys.* **2012**, *63*, 223−234.
(24) De Feo, C. J.; Aller, S. G.; Siluvai, G. S.; Blackburn, N. J.; Unger, V. M. *Proc. Natl. Acad. Sci. U. S. A.* **2009**, *106*, 4237−4242.
(25) De Feo, C. J.; Aller, S. G.; Unger, V. M. *BioMetals* **2007**, *20*, 705−716.10.1007/s10534-006-9054-7
(26) Aller, S. G.; Unger, V. M. *Proc. Natl. Acad. Sci. U. S. A.* **2006**, *103*, 3627−3632.
(27) Puig, S.; Lee, J.; Lau, M.; Thiele, D. J. *J. Biol. Chem.* **2002**, *277*, 26021−26030.
(28) Eisses, J. F.; Kaplan, J. H. *J. Biol. Chem.* **2002**, *277*, 29162−29171.
(29) Lee, J.; Pena, M. M. O.; Nose, Y.; Thiele, D. J. *J. Biol. Chem.* **2002**, *277*, 4380−4387.
(30) Haas, K. L.; Putterman, A. B.; White, D. R.; Thiele, D. J.; Franz, K. J. *J. Am. Chem. Soc.* **2011**, *133*, 4427−4437.
(31) Rubino, J. T.; Riggs-Gelasco, P.; Franz, K. J. *JBIC, J. Biol. Inorg. Chem.* **2010**, *15*, 1033−1049.
(32) Jiang, J. F.; Nadas, I. A.; Kim, M. A.; Franz, K. J. *Inorg. Chem.* **2005**, *44*, 9787−9794.
(33) Cole, C.; Barber, J. D.; Barton, G. J. *Nucleic Acids Res.* **2008**, *36*, W197−W201.
(34) Puig, S.; Thiele, D. J. *Curr. Opin. Chem. Biol.* **2002**, *6*, 171−180.
(35) Himes, R. A.; Park, G. Y.; Barry, A. N.; Blackburn, N. J.; Karlin, K. D. *J. Am. Chem. Soc.* **2007**, *129*, 5352−5353.
(36) Himes, R. A.; Park, G. Y.; Siluvai, G. S.; Blackburn, N. J.; Karlin, K. D. *Angew. Chem., Int. Ed.* **2008**, *47*, 9084−9087.
(37) Peck, K. L.; Clewett, H. S.; Schmitt, J. C.; Shearer, J. *Chem. Commun.* **2013**, *49*, 4797−4799.
(38) Shearer, J.; Szalai, V. A. *J. Am. Chem. Soc.* **2008**, *130*, 17826−17835.
(39) Shenberger, Y.; Shimshi, A.; Ruthstein, S. *J. Phys. Chem. B* **2015**, *119*, 4824−4830.
(40) Du, X.; Li, H.; Wang, X.; Liu, Q.; Ni, J.; Sun, H. *Chem. Commun. (Cambridge, U. K.)* **2013**, *49*, 9134−9136.
(41) Knutson, M. D. *Nutr. Rev.* **2007**, *65*, 335−340.
(42) Gomes, I. M.; Maia, C. J.; Santos, C. R. *Mol. Cancer Res.* **2012**, *10*, 573−587.
(43) Lonnerdal, B. *Am. J. Clin. Nutr.* **2008**, *88*, 846S−850S.
(44) Ohgami, R. S.; Campagna, D. R.; McDonald, A.; Fleming, M. D. *Blood* **2006**, *108*, 1388−1394.
(45) Scheiber, I. F.; Mercer, J. F. B.; Dringen, R. *Neurochem. Int.* **2010**, *56*, 451−460.
(46) Harford, C.; Sarkar, B. *Acc. Chem. Res.* **1997**, *30*, 123−130.
(47) Sankararamakrishnan, R.; Verma, S.; Kumar, S. *Proteins: Struct., Funct., Genet.* **2005**, *58*, 211−221.
(48) Sovago, I.; Osz, K. *Dalton Trans.* **2006**, 3841−3854.
(49) Burke, S. K.; Xu, Y. L.; Margerum, D. W. *Inorg. Chem.* **2003**, *42*, 5807−5817.
(50) Pace, C. N.; Vajdos, F.; Fee, L.; Grimsley, G.; Gray, T. *Protein Sci.* **1995**, *4*, 2411−2423.
(51) Xiao, Z.; Loughlin, F.; George, G. N.; Howlett, G. J.; Wedd, A. G. *J. Am. Chem. Soc.* **2004**, *126*, 3081−3090.
(52) Faller, P.; Hureau, C.; Dorlet, P.; Hellwig, P.; Coppel, Y.; Collin, F.; Alies, B. *Coord. Chem. Rev.* **2012**, *256*, 2381−2396.
(53) Williams-Smith, D. L.; Bray, R. C.; Barber, M. J.; Tsopanakis, A. D.; Vincent, S. P. *Biochem. J.* **1977**, *167*, 593−600.
(54) Sokolowska, M.; Bal, W. *J. Inorg. Biochem.* **2005**, *99*, 1653−1660.
(55) Hegetschweiler, K.; Saltman, P. *Inorg. Chem.* **1986**, *25*, 107−109.
(56) George, M. J. *J. Synchrotron Radiat.* **2000**, *7*, 283−286.
(57) Cramer, S. P.; Tench, O.; Yocum, M.; George, G. N. *Nucl. Instrum. Methods Phys. Res., Sect. A* **1988**, *266*, 586−591.
(58) George, G. N.; Pickering, I. J. 2001, EXAFSPAK, http://www-ssrl.slac.stanford.edu/exafspak.html.
(59) Pushie, M. J.; Doonan, C. J.; Moquin, K.; Weiner, J. H.; Rothery, R.; George, G. N. *Inorg. Chem.* **2011**, *50*, 732−740.
(60) Rehr, J. J.; Deleon, J. M.; Zabinsky, S. I.; Albers, R. C. *J. Am. Chem. Soc.* **1991**, *113*, 5135−5140.
(61) Deleon, J. M.; Rehr, J. J.; Zabinsky, S. I.; Albers, R. C. *Phys. Rev. B: Condens. Matter Mater. Phys.* **1991**, *44*, 4146−4156.
(62) Frisch, M. J.; Trucks, G. W.; Schlegel, H. B.; Scuseria, G. E.; Robb, M. A.; Cheeseman, J. R.; Scalmani, G.; Barone, V.; Mennucci, B.; Petersson, G. A.; Nakatsuji, H.; Caricato, M.; Li, X.; Hratchian, H. P.; Izmaylov, A. F.; Bloino, J.; Zheng, G.; Sonnenberg, J. L.; Hada, M.; Ehara, M.; Toyota, K.; Fukuda, R.; Hasegawa, J.; Ishida, M.; Nakajima, T.; Honda, Y.; Kitao, O.; Nakai, H.; Vreven, T.; Montgomery Jr., J. A.; Peralta, J. E.; Ogliaro, F.; Bearpark, M. J.; Heyd, J.; Brothers, E. N.; Kudin, K. N.; Staroverov, V. N.; Kobayashi, R.; Normand, J.; Raghavachari, K.; Rendell, A. P.; Burant, J. C.; Iyengar, S. S.; Tomasi, J.; Cossi, M.; Rega, N.; Millam, N. J.; Klene, M.; Knox, J. E.;

DOI: 10.1021/acs.inorgchem.5b01162
Inorg. Chem. 2015, 54, 8544−8551

Cross, J. B.; Bakken, V.; Adamo, C.; Jaramillo, J.; Gomperts, R.; Stratmann, R. E.; Yazyev, O.; Austin, A. J.; Cammi, R.; Pomelli, C.; Ochterski, J. W.; Martin, R. L.; Morokuma, K.; Zakrzewski, V. G.; Voth, G. A.; Salvador, P.; Dannenberg, J. J.; Dapprich, S.; Daniels, A. D.; Farkas, Ö.; Foresman, J. B.; Ortiz, J. V.; Cioslowski, J.; Fox, D. J. *Gaussian09*, revision D.01; Gaussian, Inc.: Wallingford, CT, 2009.
(63) Scalmani, G.; Frisch, M. J. *J. Chem. Phys.* **2010**, *132*, 15.
(64) Pushie, M. J.; Nienaber, K. H.; McDonald, A.; Millhauser, G. L.; George, G. N. *Chem. - Eur. J.* **2014**, *20*, 9770−9783.
(65) Allen, F. *Acta Crystallogr., Sect. B: Struct. Sci.* **2002**, *58*, 380−388.
(66) Bruno, I. J.; Cole, J. C.; Edgington, P. R.; Kessler, M.; Macrae, C. F.; McCabe, P.; Pearson, J.; Taylor, R. *Acta Crystallogr., Sect. B: Struct. Sci.* **2002**, *58*, 389−397.
(67) Wang, L. Y.; Chambron, J. C.; Espinosa, E. *New J. Chem.* **2009**, *33*, 327−336.
(68) Kau, L. S.; Spirasolomon, D. J.; Pennerhahn, J. E.; Hodgson, K. O.; Solomon, E. I. *J. Am. Chem. Soc.* **1987**, *109*, 6433−6442.
(69) Feaga, H. A.; Maduka, R. C.; Foster, M. N.; Szalai, V. A. *Inorg. Chem.* **2011**, *50*, 1614−1618.

DOI: 10.1021/acs.inorgchem.5b01162
Inorg. Chem. 2015, 54, 8544−8551